J Mater Sci (2012) 47:1054–1058
DOI 10.1007/s10853-011-5894-9

Ibuprofen loaded porous calcium phosphate nanospheres for skeletal drug delivery system

Fengwei Shao · Lin Liu · Kejie Fan · Yurong Cai · Juming Yao

Received: 18 June 2011 / Accepted: 22 August 2011 / Published online: 7 September 2011

Abstract Porous calcium phosphate nanospheres were successfully fabricated by a simple sonochemical method, and used as a drug carrier of ibuprofen. Morphology, structure, ibuprofen storage capacity, and release rate of the calcium phosphate nanospheres were characterized using FE-SEM, TEM, Nitrogen adsorption, XRD, FTIR, and UV–vis adsorption spectroscopies. Results showed the obtained calcium phosphate nanospheres held a porous structure with an average diameter of 48.9 ± 17.42 nm. Moreover, the porous nanospheres possessed an adjustable load amount and release rate for ibuprofen by changing drug concentrations during the drug loading process. In addition, the effects of size and dispersancy of porous spheres on drug release rate were discussed, which was found that larger or agglomerate porous spheres could delay drug release process. This study indicated that porous calcium phosphate nanospheres were a perfect drug carrier for ibuprofen, which has potential application for the therapy of skeletal disease.

Introduction

In the last decade, several new forms of drug delivery systems (DDS) have emerged for clinical use, including capsules, liposomes, microparticles, nanoparticles, and polymers, but their biocompatibility, biodegradability, drug delivery/release behaviors, and new drug dosage for skeletal drug delivery still need more attentions [1]. For example, because the routine use of systemic antibiotics and anti-inflammatory drugs after bone operation for prophylaxis in the postoperative complications are not adequate to alleviate these ailments due to the poor perfusion of diseased bone tissue and are also responsible for drug toxicity to other sites, delivering the drug directly to skeletal tissue is a crucial requirement through self-setting cement, thereby improving the therapeutic effectiveness of drugs in the bone diseases. This new drug delivery method was introduced as skeletal drug delivery system (SDDS) by Bucholz and Engelbrecht [2].

Calcium phosphate (CaP) is an ideal skeletal drug carrier and bone substitute in the biomedical application due to its powerful adsorption ability, excellent biocompatibility, and osteoconductibility [3, 4]. As a drug carrier, the self-setting ability of this calcium phosphate in vivo allows cement implantation. Its chemical and structural similarity to biological apatites make it perfectly fit to the implant site of skeletal system. So the effect of various morphologies and surface properties of CaP on the load ability of antibiotics [5–8], anticancer drugs [9, 10], and proteins [11–13] is a hot issue. However, very few drug carrier of CaP has been used in clinic because of its poor injectability, poor stability, and unreasonable release speed of drug.

Ibuprofen (IBU, $C_{13}H_{18}O_2$), an analgesic and anti-inflammatory drug, has been chosen as a model drug in this study due to its short biological half-life and good pharmacological activity, which could be employed in the skeletal regeneration. Moreover, this drug could contribute to the local treatment of inflammation following surgery or to the treatment of bone loss in periodontitis [14].

Electronic supplementary material The online version of this article (doi:10.1007/s10853-011-5894-9) contains supplementary material, which is available to authorized users.

F. Shao · L. Liu · K. Fan · Y. Cai · J. Yao (✉)
The Key Laboratory of Advanced Textile Materials and Manufacturing Technology of Ministry of Education, College of Materials and Textile, Zhejiang Sci-Tech University, Xiasha Higher Education Park, Hangzhou 310018, China
e-mail: yaoj@zstu.edu.cn

In this study, porous CaP nanospheres were fabricated by the sonochemical method [15, 16]. The IBU was then loaded into the CaP nanospheres through a solvent volatilization method under vacuum. The structure, IBU encapsulation, and release properties of IBU for these nanospheres were then investigated.

Materials and methods

Materials

IBU, a white crystalline powder with the purity of 99%, was purchased from Alfa Aesar Co., Ltd. (Tianjin, China). All other chemical reagents, including $CaCl_2$, $Na_2HPO_4 \cdot 12H_2O$, $NH_4 \cdot OH$, NaCl, KCl, and KH_2PO_4 used for CaP synthesis and phosphate buffer saline (PBS) preparation were of analytical grade and purchased from Mike Chemical Agents Co., Ltd. (Hangzhou, China).

Methods

Synthesis of porous CaP nanospheres

Porous CaP nanospheres were fabricated by chemical coprecipitation in an aqueous solution. In brief, the pH value of 720 mL $CaCl_2$ aqueous solution (5.6 mM) was adjusted to 9.5 by the addition of $NH_4 \cdot OH$ aqueous solution (1 M) with stirring at the speed of 500 rpm for 30 min. And then 80 mL Na_2HPO_4 aqueous solution (30 mM) was added drop-wise under an ultrasonic condition. After another 8 min stirring, precipitates were collected by centrifugation at 7000 rpm, washed with deionized water for three times. Obtained precipitates were vacuum-dried and named as pCaP.

Loading of IBU

IBU was adsorbed onto the particles surface or encapsulated into the particles porous channels through a solvent volatilization method under vacuum. In a typical process, IBU was dissolved in a conical flask containing 10 mL ethanol, and IBU concentration was varied from 7.5, 15 to 30 mg/mL, respectively. After 1 g of pCaP was added into the IBU solution, the conical flask was placed into the vacuum for 4 days at 40 °C, and low-temperature setting of IBU could keep biological activity of the drug. Obtained samples were named as CaP-IBU7.5, CaP-IBU15, and CaP-IBU30 corresponding to the increased order of IBU concentration.

Morphologic and chemical characterizations

CaP particles with and without IBU were dispersed in the distilled water and then dropped onto the surface of silica flake for FE-SEM observation using a field emission scanning electron microscope (SE) (S4800, Hitachi) at 1 kV. The pCaP samples were investigated using a TEM (JEM-1230, JEOL) at 80 kV after were dispersed in distilled water and dropped onto carbon-coated copper grids. Nitrogen adsorption method was applied to characterize the pore diameter distribution of pCaP samples using a surface area and pore size analyzer (F-Sorb 3400, Gold Application). Samples were heated at 90 °C for 2 h under vacuum before test in order to remove absorbed vapor and air. The chemical composition of samples with and without IBU was analyzed with an X-ray powder diffractometer (ARL X'TRA, Thermo Electron) using a monochromatic CuKα radiation ($\lambda = 1.54056$ nm) in a range of $2\theta = 10°$–$90°$ with a step of 0.04°. Samples were mixed with KBr in a mass ratio of 1:150 for the FT-IR observation, which were recorded on an attenuated total reflection fourier transform infrared instrument (Nicolet 5700, Thermo Electron) in the range of 400–4000 cm^{-1} with a resolution of 4 cm^{-1}. Thermogravimetry of the samples was performed by a thermogravimetry analyzer (Pyris Diamond, PerkinElmer Inc.).

In vitro drug release kinetics

In vitro release studies of IBU from CaP nanospheres were performed according to the modified Chinese Pharmacopoeia (ChP) model for tablet dissolution test. In a typical test, 100 mg IBU loaded CaP was introduced in 200 mL … (pH = 7.4) at the paddle rotation speed of 100 rpm, 25 °C. At the time points of 0, 0.5, 1, 2, 3, 5, and 8 h, 2 mL solution was withdrawn, respectively, and the IBU content in supernatant was determined by UV–vis absorption spectroscopy at 264 nm. Meanwhile, 2 mL fresh PBS prewarmed at 25 °C was replenished into the release medium to maintain its constant volume for the next release process. Calculation of the corrected concentration of released IBU was based on the following equation [17]:

$$C_{t\mathrm{cor}} = C_t + \frac{v}{V}\sum_{0}^{t-1} C_t \tag{1}$$

where $C_{t\mathrm{cor}}$ is the corrected concentration at time t, C_t is the apparent concentration at time t, v is the volume of sample taken, and V is the total volume of dissolution medium. Release studies were performed in triplicate.

Different specific surface area and pore structure could be elicited due to formation of particle aggregates, by which drug-loaded and released ability of particles would be changed. But a combination of particle unit and its aggregate will take effect on organism after the material is used in vivo. So it is necessary to understand drug release behavior of aggregates as well particles. Furthermore, the drug release rate could be controlled through selecting and/or combining

drug-loaded aggregates with different sizes. So in order to study the effects of size and dispersancy of porous spheres on drug release rate, particles of CaP-IBU15 were selected by standard sieves with the mesh of 65 and 120, and three kinds of particles with size of <120, 120–230, and >230 μm were obtained. Release behaviors of IBU from them were investigated by the method as mentioned above.

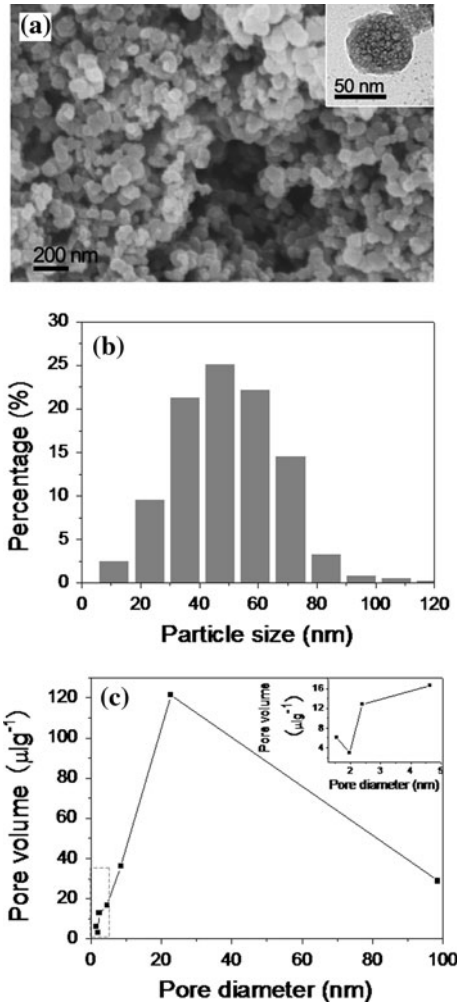

Fig. 1 **a** FE-SEM image, **b** particle size distribution, and **c** pore diameter distribution of pCaP particles. The *inset* in (**a**) shows the TEM image of pCaP, and the *inset* in (**c**) shows the small pore diameter distribution

Results and discussion

Morphology

Typical morphology and size of pCaP was showed in Fig. 1a, which clearly indicated the pCaP had an approximately spherical shape and wide size distribution. The average particles size was 48.89 ± 17.42 nm according to the statistical analysis of 366 particles in an area of 3×3 μm^2 (Fig. 1b). The inserted image in Fig. 1a showed that the pCaP had a microporous structure. Nitrogen adsorption and desorption analysis was then applied based on BJH (Barrett–Joyner–Halenda) method [18], which showed that the pore size distribution of pCaP was centered at about 20 nm, and the average pore diameter was 26 nm (Fig. 1c). To take into account of the structural integrity and 50 nm diameter of particles, the macropores had been formed mainly among particles. Porous structure of pCaP had the potential advantage for the drug loading. Figure 2 showed the morphologies of IBU loaded CaP particles by FE-SEM, including CaP-IBU7.5, CaP-IBU15, and CaP-IBU30, respectively. The results indicated that all three samples were spherical, and the adsorption of IBU layer led to a slight increase of particles size.

Chemical composition

Figure 3 showed the XRD patterns and FTIR spectra of pCaP, IBU loaded samples, and pure IBU. The broadening and overlap of peaks appeared in XRD patterns (Fig. 3a) of samples suggested their poor crystallinity. We speculated that the composite of amorphous calcium phosphate and

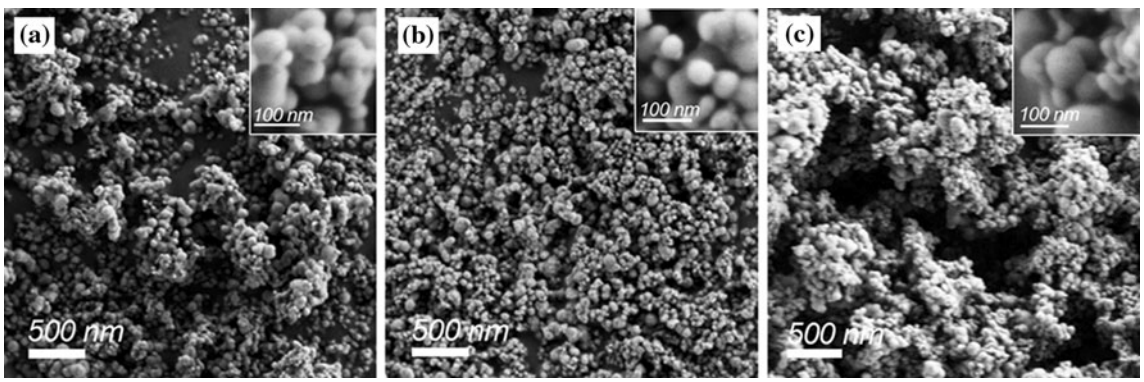

Fig. 2 FE-SEM images **a** of CaP-IBU7.5, **b** CaP-IBU15, and **c** CaP-IBU30, respectively

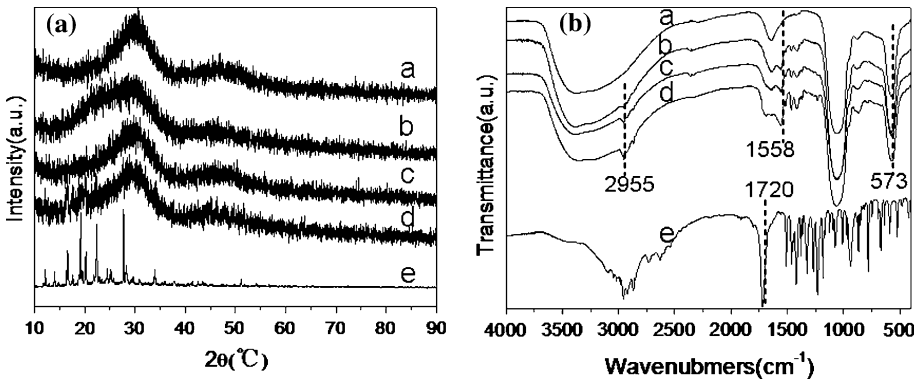

Fig. 3 **a** XRD patterns and **b** FTIR spectra of *a* pCaP, *b* CaP-IBU7.5, *c* CaP-IBU15, *d* CaP-IBU30, and *e* IBU, respectively

IBU had been fabricated. But the IBU diffraction peaks were not found in the IBU loaded samples, probably due to its noncrystal phase of IBU in the particles [19]. The FTIR spectra (Fig. 3b) of pCaP and IBU loaded CaP samples showed the absorption bands at around 573 and 1059 cm^{-1} corresponding to the PO_4^{3-} in the CaP samples, while the broad band appeared around 3384 cm^{-1} was ascribed to the OH group. Moreover, the spectra of IBU loaded CaP samples showed the additional peaks at around 2955–2868 cm^{-1}, which were assigned to the symmetric and asymmetric stretching vibrations of $–CH_x$ groups in the IBU alkyl chains. The band corresponding to υ (C=O) was shifted from 1720 to 1558 cm^{-1}, suggesting there was a bonding between IBU molecules and CaP. In addition, the characteristic vibrations of C=C modes and C–C modes of the aromatic rings were observed at 1463 and 1418 cm^{-1}, respectively, which became more intensive in the spectrum of CaP-IBU30 due to the more IBU loaded in CaP.

Figure 4 showed TGA curves of pCaP and IBU loaded CaP samples from 40 to 700 °C. The main weight loss appeared below 350 °C for all of the samples. The total weight lose at 700 °C was 11% for pCaP, but increased to 22, 26, and 34% for CaP-IBU7.5, CaP-IBU15, and CaP-IBU30, respectively. The high weight loss for IBU loaded CaP samples was due to the decomposition of loaded IBU. The increase of weight loss in order of CaP-IBU7.5, CaP-IBU15, and CaP-IBU30 implied that the loaded amount of IBU was controlled by regulating its initial concentration of IBU.

IBU release

UV–vis absorption spectrum of pure IBU in PBS showed a maximum absorption at 264 nm. Based on the absorbance at 264 nm of the solution with known concentration of IBU, a calibration curve was prepared (see Supplemental Materials). So that, the IBU concentrations in the supernatant released from drug loaded CaP samples were determined. Figure 5 showed the release behavior of the IBU loaded CaP samples in PBS. All the samples had a

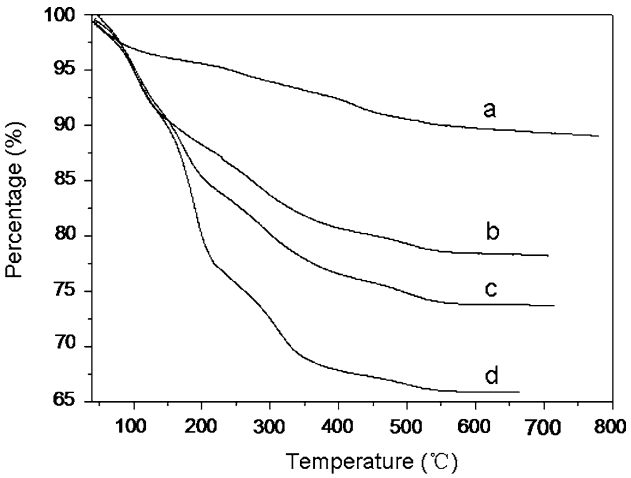

Fig. 4 TGA curves of *a* pCaP, *b* CaP-IBU7.5, *c* CaP-IBU15, and *d* CaP-IBU30, respectively

quick initial release rate of 76, 152, and 186 μg/h within initial 40 min corresponding to CaP-IBU7.5, CaP-IBU15, and CaP-IBU30, respectively, because it was more easier for adsorbed IBU on the surface of particle released from the particles. A slower release rate was then available, which was decreased to 0.857, 2.75, and 3.29 μg/h for CaP-IBU7.5, CaP-IBU15, and CaP-IBU30, respectively.

Figure 6 showed the cumulative curves of IBU released from CaP-IBU15 with three kinds of particle size, i.e., <120, 120–230, and >230 μm. Interestingly, the release rate of IBU from CaP-IBU15 could be modulated by narrowing the particle size distribution. Although they had a large initial release rate, all of three samples had a sustained IBU release profile. After the large initial release stage, their release rates were 4.36, 2.50, and 1.61 μg/h for CaP-IBU15 with the size of <120, 120–230, and >230 μm, respectively. This result may bring some new ideas for controlled drug release system, because if known release rates of different particle aggregates, drug release rate may be controlled through uniformly mixing two or three kinds of particle aggregates at a proper proportion. It is fairly to speculate that the initial release stage was attributed to the

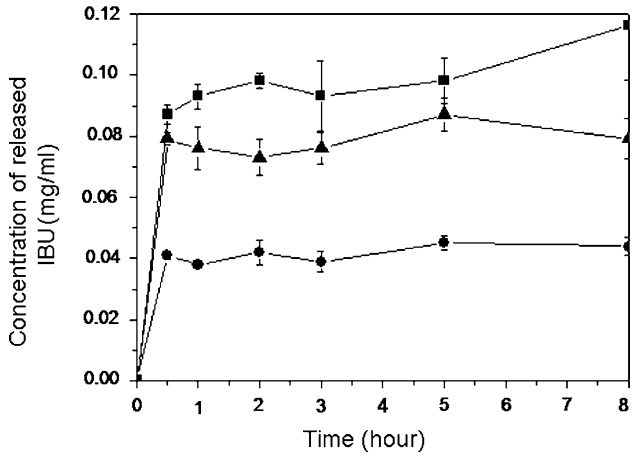

Fig. 5 Comparative cumulative curves of IBU concentration released from CaP-IBU7.5 (*filled circle*), CaP-IBU15 (*filled triangle*), and CaP-IBU30 (*filled square*)

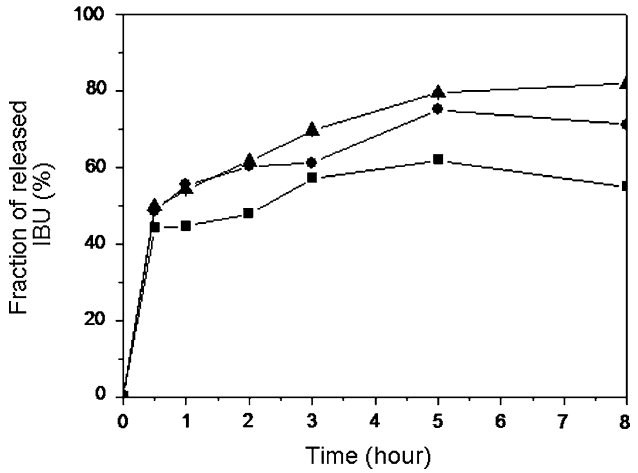

Fig. 6 Comparative cumulative percentage curves of IBU released from CaP-IBU15 with varied particles size of <120 μm (*filled triangle*), 120–230 μm (*filled circle*), and >230 μm (*filled square*)

surface adsorption of IBU, while the second sustained release stage should be assigned to the release of encapsulated IBU in the porous channels on the surface of particles or among the particles.

Conclusions

Porous CaP nanospheres were successfully fabricated by a simple sonochemical method and IBU was loaded onto the nanospheres through a solvent volatilization method under vacuum. The porosity made it a high drug loading efficiency, more resorbable, and more osteoconductive, while the low crystallinity of CaP may led it more soluble and degradable than sintered CaP. Different amount of IBU could be encapsulated into the internal porous structure or absorbed onto the surface of pCaP by changing IBU concentration in ethanol. Moreover, the IBU release behavior could be regulated by changing the particle size. So that, porous CaP nanosphere is an ideal drug carrier for IBU and may has potential application for the therapy of skeletal disease.

Acknowledgements This study is financially supported by the Program for New Century Excellent Talents in University (NCET070763), Special Programm of National Natural Science Foundation of China (Grant21041003), and Zhejiang Natural Science Foundation of China (Y4090416).

References

1. Allen TM, Cullis PR (2004) Science 303:1818
2. Buchholz HW, Engelbrecht H (1970) Chirurg 41:511
3. LeGeros RZ (2008) Chem Rev 108:4742
4. Loku K, Kawachi G, Sasaki S, Fujimori H, Goto S (2006) J Mater Sci 41(5):1341. doi:10.1007/s10853-006-7338-5
5. Itokazu M, Yang W, Aoki T, Ohara A, Kato N (1998) Biomaterials 19:817
6. Soriano I, Évora C (2000) J Control Release 68:121
7. Murugan R, Ramakrishna S (2006) J Mater Sci 41(13):4343. doi:10.1007/s10853-006-6157-z
8. Makarov C, Gotman I, Radin S, Ducheyne P, Gutmanas EY (2009) J Mater Sci 45(23):6320. doi:10.1007/s10853-010-4444-1
9. Uchida DA, Shinto Y, Araki N, Ono K (1992) J Orthopaed Res 10(3):440
10. Iafisco M, Palazzo B, Marchetti M, Margiotta N, Ostuni R, Natile G, Morpurgo M, Gandin V, Marzano C, Roveri N (2009) J Mater Chem 19:8385
11. Alam MI, Asahina I, Ohmamiuda K, Takahashi K, Yokota S, Enomoto S (2001) Biomaterials 22:1643
12. Ho ML, Fu YC, Wang GJ, Chen HT, Chang JK, Tsai TH, Wang CK (2008) J Control Release 128:142
13. Matsumoto T, Okazaki M, Inoue M, Yamaguchi S, Kusunose T, Toyonaga T, Hamada Y, Takahashi J (2004) Biomaterials 25: 3807
14. Chevalier E, Viana M, Cazalbou S, Makein L, Dubois J, Chulia D (2010) Acta Biomater 6:266
15. Dhas NA, Suslick KS (2005) J Am Chem Soc 127(8):2368
16. Cai YR, Pan HH, Xu XR, Hu QH, Li L, Tang RK (2007) Chem Mater 19(13):3081
17. Fisher KA, Huddersman KD, Taylor MJ (2003) Chem Eur J 9: 5873
18. Leslaw J, Teresa F, Krystyna W (2002) J Food Eng 54(2):103
19. Otsuka M, Matsuda Y, Suwa Y, Fox JL, Higuchi T (1994) J Pharm Sci 83:611